Two MHz tunable non collinear optical parametric amplifiers with pulse durations down to 6 fs

Julien Nillon,[1,2,*] Olivier Crégut,[1] Christian Bressler,[2,3] and Stefan Haacke[1]

[1]*Institut de Physique et Chimie des Matériaux de Strasbourg, UMR 7504 CNRS, Université de Strasbourg, 67034 Strasbourg, France*
[2]*European XFEL, Albert Einstein Ring 19, 22761 Hamburg, Germany*
[3]*The Hamburg Centre for Ultrafast Imaging, Luruper Chaussee 149, 22761 Hamburg, Germany*
[*]*nillon@ipcms.unistra.fr*

Abstract: We report on the development of a 2 MHz non collinear optical parametric amplifier (NOPA) for high repetition rate time resolved X-ray or optical spectroscopy. Our modular and very flexible device is pumped by the second and third harmonics of a commercial femtosecond Ytterbium-doped fiber laser. The amplified pulses are tunable from 520 nm to 1000 nm with pulse durations between 15 and 30 fs over the full tuning range. The same setup is also suitable for broadband amplification and we demonstrate the generation of 6 fs pulses at a central wavelength of 850 nm as well as the generation of a broadband spectrum supporting 4.2 fs transform limited pulse duration at a central wavelength of 570 nm. Very high stability and compactness is achieved thanks to an optimized mechanical design.

OCIS codes: (060.2320) Fiber optics amplifiers and oscillators; (190.4970) Parametric oscillators and amplifiers; (190.7110) Ultrafast nonlinear optics; (320.5520) Pulse compression; (320.7080) Ultrafast devices.

References and links

1. G. Cerullo and S. De Silvestri, "Ultrafast optical parametric amplifiers," Rev. Sci. Instrum. **74**(1), 1–18 (2003).
2. G. M. Gale, M. Cavallari, T. J. Driscoll, and F. Hache, "Sub-20-fs tunable pulses in the visible from an 82-MHz optical parametric oscillator," Opt. Lett. **20**(14), 1562–1564 (1995).
3. T. Wilhelm, J. Piel, and E. Riedle, "Sub-20-fs pulses tunable across the visible from a blue-pumped single-pass noncollinear parametric converter," Opt. Lett. **22**(19), 1494–1496 (1997).
4. A. Shirakawa and T. Kobayashi, "Noncollinearly phase-matched femtosecond optical parametric amplification with a 2000 cm−1 bandwidth," Appl. Phys. Lett. **72**(2), 147–149 (1998).
5. M. Beutler, M. Ghotbi, F. Noack, D. Brida, C. Manzoni, and G. Cerullo, "Generation of high-energy sub-20 fs pulses tunable in the 250-310 nm region by frequency doubling of a high-power noncollinear optical parametric amplifier," Opt. Lett. **34**(6), 710–712 (2009).
6. C. Ventalon, J. M. Fraser, J.-P. Likforman, D. M. Villeneuve, P. B. Corkum, and M. Joffre, "Generation and complete characterization of intense mid-infrared ultrashort pulses," J. Opt. Soc. Am. B **23**(2), 332–340 (2006).
7. G. Cerullo, M. Nisoli, S. Stagira, and S. De Silvestri, "Sub-8-fs pulses from an ultrabroadband optical parametric amplifier in the visible," Opt. Lett. **23**(16), 1283–1285 (1998).
8. C. Aguergaray, O. Schmidt, J. Rothhardt, D. Schimpf, D. Descamps, S. Petit, J. Limpert, and E. Cormier, "Ultra-wide parametric amplification at 800 nm toward octave spanning," Opt. Express **17**(7), 5153–5162 (2009).
9. C. Vozzi, C. Manzoni, F. Calegari, E. Benedetti, G. Sansone, G. Cerullo, M. Nisoli, S. De Silvestri, and S. Stagira, "Characterization of a high-energy self-phase-stabilized near-infrared parametric source," J. Opt. Soc. Am. B **25**(7), B112–B117 (2008).
10. A. Baltuška, T. Fuji, and T. Kobayashi, "Visible pulse compression to 4 fs by optical parametric amplification and programmable dispersion control," Opt. Lett. **27**(5), 306–308 (2002).
11. K. Okamura and T. Kobayashi, "Octave-spanning carrier-envelope phase stabilized visible pulse with sub-3-fs pulse duration," Opt. Lett. **36**(2), 226–228 (2011).
12. F. A. Lima, C. J. Milne, D. C. V. Amarasinghe, M. H. Rittmann-Frank, R. M. van der Veen, M. Reinhard, V.-T. Pham, S. Karlsson, S. L. Johnson, D. Grolimund, C. Borca, T. Huthwelker, M. Janousch, F. van Mourik, R. Abela, and M. Chergui, "A high-repetition rate scheme for synchrotron-based picosecond laser pump/x-ray probe experiments on chemical and biological systems in solution," Rev. Sci. Instrum. **82**(6), 063111 (2011).

#209302 - $15.00 USD Received 31 Mar 2014; revised 30 May 2014; accepted 30 May 2014; published 11 Jun 2014

13. F. Röser, T. Eidam, J. Rothhardt, O. Schmidt, D. N. Schimpf, J. Limpert, and A. Tünnermann, "Millijoule pulse energy high repetition rate femtosecond fiber chirped-pulse amplification system," Opt. Lett. **32**(24), 3495–3497 (2007).
14. J. Rothhardt, S. Hädrich, D. N. Schimpf, J. Limpert, and A. Tünnermann, "High repetition rate fiber amplifier pumped sub-20 fs optical parametric amplifier," Opt. Express **15**(25), 16729–16736 (2007).
15. C. Schriever, S. Lochbrunner, P. Krok, and E. Riedle, "Tunable pulses from below 300 to 970 nm with durations down to 14 fs based on a 2 MHz ytterbium-doped fiber system," Opt. Lett. **33**(2), 192–194 (2008).
16. C. Homann, C. Schriever, P. Baum, and E. Riedle, "Octave wide tunable uv-pumped NOPA: pulses down to 20 fs at 0.5 MHz repetition rate," Opt. Express **16**(8), 5746–5756 (2008).
17. H. Fattahi, C. Y. Teisset, O. Pronin, A. Sugita, R. Graf, V. Pervak, X. Gu, T. Metzger, Z. Major, F. Krausz, and A. Apolonski, "Pump-seed synchronization for Mhz repetition rate, high-power optical parametric chirped pulse amplification," Opt. Express **20**(9), 9833–9840 (2012).
18. J. Rothhardt, S. Demmler, S. Hädrich, J. Limpert, and A. Tünnermann, "Octave-spanning OPCPA system delivering CEP-stable few-cycle pulses and 22 W of average power at 1 MHz repetition rate," Opt. Express **20**(10), 10870–10878 (2012).
19. A. Harth, M. Schultze, T. Lang, T. Binhammer, S. Rausch, and U. Morgner, "Two-color pumped OPCPA system emitting spectra spanning 1.5 octaves from VIS to NIR," Opt. Express **20**(3), 3076–3081 (2012).
20. M. Krebs, S. Hädrich, S. Demmler, J. Rothhardt, A. Zaïr, L. Chipperfield, J. Limpert, and A. Tünnermann, "Towards isolated attosecond pulses at megahertz repetition rates," Nat. Photonics **7**(7), 555–559 (2013).
21. M. Bradler, P. Baum, and E. Riedle, "Femtosecond continuum generation in bulk laser host materials with sub-μJ pump pulses," Appl. Phys. B **97**(3), 561–574 (2009).
22. J. Bromage, J. Rothhardt, S. Hädrich, C. Dorrer, C. Jocher, S. Demmler, J. Limpert, A. Tünnermann, and J. D. Zuegel, "Analysis and suppression of parasitic processes in noncollinear optical parametric amplifiers," Opt. Express **19**(18), 16797–16808 (2011).
23. J. Rothhardt, S. Demmler, S. Hädrich, T. Peschel, J. Limpert, and A. Tünnermann, "Thermal effects in high average power optical parametric amplifiers," Opt. Lett. **38**(5), 763–765 (2013).
24. D. N. Schimpf, J. Rothhardt, J. Limpert, A. Tünnermann, and D. C. Hanna, "Theoretical analysis of the gain bandwidth for noncollinear parametric amplification of ultrafast pulses," J. Opt. Soc. Am. B **24**(11), 2837–2846 (2007).
25. R. L. Fork, O. E. Martinez, and J. P. Gordon, "Negative dispersion using pairs of prisms," Opt. Lett. **9**(5), 150–152 (1984).
26. V. Pervak, "Recent development and new ideas in the field of dispersive multilayer optics," Appl. Opt. **50**(9), C55–C61 (2011).
27. M. Emons, A. Steinmann, T. Binhammer, G. Palmer, M. Schultze, and U. Morgner, "Sub-10-fs pulses from a MHz-NOPA with pulse energies of 0.4 microJ," Opt. Express **18**(2), 1191–1196 (2010).
28. S. Maillot, A. Carvalho, J. P. Vola, C. Boudier, Y. Mély, S. Haacke, and J. Léonard, "Out-of-equilibrium biomolecular interactions monitored by picosecond fluorescence in microfluidic droplets," Lab Chip **14**(10), 1767–1774 (2014).

1. Introduction

Ultrafast spectroscopy and non-linear imaging techniques require femtosecond pulses with excitation wavelengths matching the absorption bands of the studied material system. Providing continuously tunable emission throughout the visible and infrared, Optical Parametric Amplification (OPA) has proven to be a very attractive solution to fill the gaps between those discrete laser wavelengths, with tunable broadband amplification being possible in non-collinear OPA's [1–4]. With additional Second Harmonic Generation (SHG) or Difference Frequency Generation (DFG), the tunability could be extended from the UV to the mid-IR [5, 6], to match the excitation range of electronic and vibrational transitions of condense phase material systems.

Another interesting feature of OPA is the ability to amplify very broad spectral bandwidth up to a full octave, using some particular interaction geometries such as non-collinear amplification (NOPA) at the so-called "magic-angle" [7, 8] or amplification at degeneracy [9]. Such amplification strategies lead after compression to the generation of ultrashort pulses, down to 4 fs [10], or even 3 fs via SHG of the spatially dispersed idler beam [11]. This enables time-resolved studies with superb time resolution and fuels the generation of isolated attosecond pulses when combined with Carrier-Envelope Phase (CEP) stabilization.

There is now a growing need for higher repetition rate parametric sources in order to shorten acquisition times and increase the signal-to-noise ratio. This is very important for many applications like High orders Harmonics Generation (HHG) due to its poor conversion efficiency, or for optical pump/X-ray probe time resolved studies performed at synchrotron radiation facilities. Depending on the chosen filling pattern, the repetition rate of synchrotrons

#209302 - $15.00 USD Received 31 Mar 2014; revised 30 May 2014; accepted 30 May 2014; published 11 Jun 2014

lies in the MHz to GHz range, which means that most X-ray photons are lost when using conventional kHz OPA pumped by Titane-Sapphire lasers. Some experiments have been performed with MHz lasers recently [12] but still lack the flexibility of a tunable source.

Increasing the repetition rate of OPA systems is now possible thanks to the quickly progressing technology of ultrafast fiber lasers with for example the demonstration of mJ class high repetition rate femtosecond sources [13]. Reliable femtosecond fiber lasers are now commercially available delivering energies of several tens of microjoules at repetition rates up to 5 MHz.

There has been a lot of work in the last years to adapt the technology of parametric devices to these new MHz pumping sources. 2 MHz OPA sources have been demonstrated able to generate sub-20 fs pulses at a fixed wavelength of 800 nm [14] or tunable from 620 to 970 nm [15]. Broader tuning range has been demonstrated with a NOPA pumped with the third harmonic of a fiber laser but at a reduced repetition rate of 500 kHz [16]. Generation of 10 fs pulses at 800 nm has also been reported at a very high repetition rate of 11.5 MHz [17]. Triggered by the need for high repetition rate HHG sources, a lot of efforts have been dedicated to the development of few-cycle MHz CEP-stabilized NOPA [18, 19], eventually resulting in the first evidences of isolated attosecond pulse generation at 600 kHz [20].

Usually, parametric devices are very specialized systems designed for one specific application with fixed performances. In contrast, the present paper reports on a compact and integrated system designed to achieve the highest flexibility on every laser parameter in order to meet most users' demands, without compromising with the state-of-the-art figures of merit. The performances of the NOPA described below are totally adjustable, with repetition rates from single shot to 2 MHz, tuning from UV to NIR and narrowband or broadband amplification. While all these parameters can be adjusted within seconds or a couple of minutes, special attention was paid to beam stability, with shot-to-shot power fluctuations of 1.3% thanks to a compact and robust mechanical design. Moreover, we demonstrate for the first time the generation at 2 MHz of two optical cycle pulses at a wavelength of 850 nm with a compact white light seeded NOPA, as well as the amplification of a broadband spectrum supporting two cycle pulses at 570 nm.

2. Two-MHz NOPA optical design

The *Tangerine* Fiber Chirped Pulse Amplifier (FCPA) from *Amplitude Systèmes* pumps our NOPA. This laser delivers a maximum output power of 20 W at the fundamental wavelength of 1030 nm, with a repetition rate tunable from 200 to 2000 kHz (pulse energy from 100 to 10 μJ) and an output pulse duration of 320 fs. It benefits from two Acousto-Optic Modulator (AOM) pulse pickers, one internal which selects the output energy, and one external which selects the repetition rate (i.e. the average power). For experiments, the internal AOM repetition rate is fixed to 2 MHz (10 μJ) to maintain a constant energy level and intensity inside the nonlinear crystals, while the external modulator is used to adjust the repetition rate from single shot to 2 MHz depending on the experiments.

The lower limit of the amplifiable spectrum in a NOPA is defined by the transparency window of the crystal used (due to absorption of the idler) as well as by the wavelength of pump. For example, when using a Beta Barium Borate (BBO) crystal as nonlinear medium, a NOPA pumped by the second harmonic (SH) of an Ytterbium-doped fiber laser at 515 nm is able to amplify wavelengths down to about 620 nm while a third harmonic (TH) pumped NOPA at 343 nm will amplify down to about 390 nm. To guarantee tunability throughout the visible spectrum we have decided to design a TH-pumped NOPA, in parallel to a SH-NOPA which has shorter pulse duration and higher energy in the NIR as shown later. Both NOPAs are seeded by the same white light continuum and we can easily switch from one to the other depending on the spectral range of interest.

The optical layout is sketched in Fig. 1. Practically, the beam enters the NOPA box through a half waveplate (HWP 1) which rotates the polarization in the vertical plane. A beam splitter (BS) reflects 80% of the total power for pump generation while the remaining power is used for white light seed generation. A module composed of two half waveplates (HWP

#209302 - $15.00 USD Received 31 Mar 2014; revised 30 May 2014; accepted 30 May 2014; published 11 Jun 2014

2&3) and a polarizing beamsplitter (PBS) is used to switch the pump from one NOPA to the other: depending on the orientation of HWP 2, the IR pump beam is either reflected to generate a 515 nm pump via SHG or transmitted to generate a 343 nm pump via THG. The polarizations of both beams are selected in order to have both pump beams horizontally polarized after harmonics generation to get type I phase-matching in the NOPAs. Moreover, an afocal lens is used to decrease the beam diameter on both arms (lenses L2 + L3 and L2 + L4) so as to achieve enough intensity in the SHG and THG crystals.

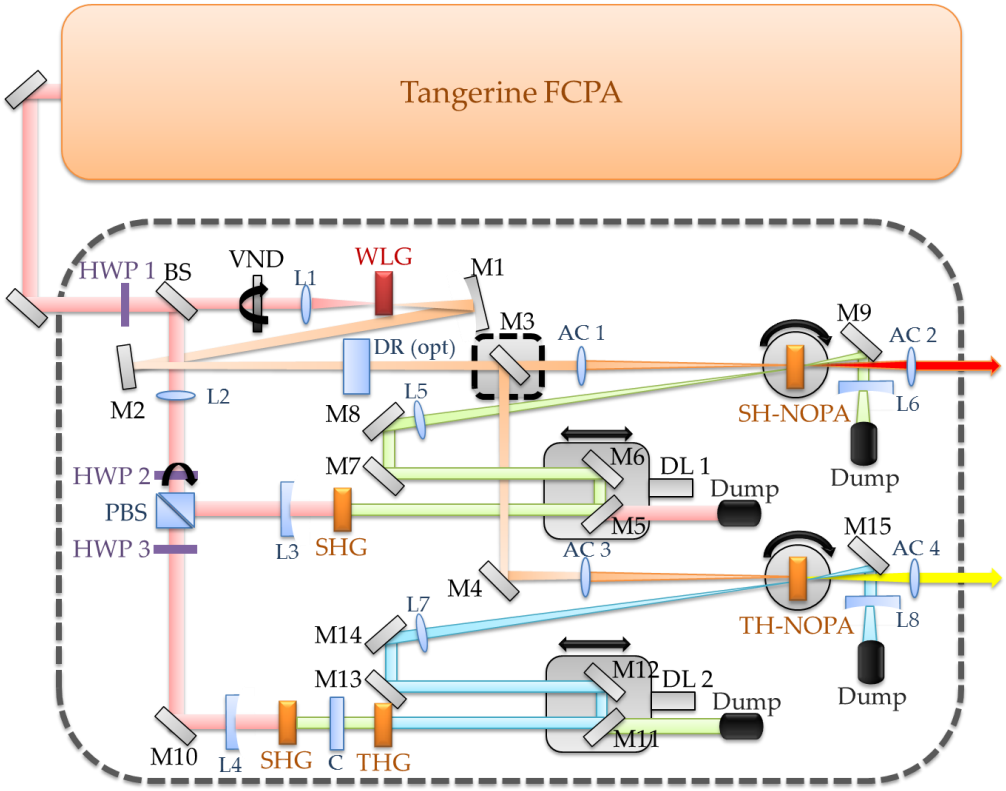

Fig. 1. Experimental setup of the 2 MHz NOPA prototype. HWP: half waveplate; BS: beam splitter; PBS: polarizing beam splitter cube; VND: variable neutral density filter; Lx: plano-convex spherical lens; WLG: white light continuum plate; Mx: mirror; AC: achromatic lens doublet; DR: dispersion rod; DL: delay line; C: calcite compensation plate.

The crystal used for SHG pump generation is a 2 mm thick type I BBO crystal cut at 23.4°. We obtain 8 W of SH radiation at 515 nm (i.e. 4 µJ, 50% efficiency).

For THG pump generation, a 1.5 mm thick type I BBO crystal cut at 23.4° is used for SHG. For THG, type II (1030.0(e) + 515.0(o) = 343.3(e)) has been selected to yield the best conversion efficiency at high repetition rate. The crystal is a 1.5 mm thick type II BBO cut at 40.1°. An additional 0.5 mm thick calcite plate cut at 45° is used for group delay compensation between SHG and THG crystals. We obtain 5 W of TH radiation at 343 nm (i.e. 2.5 µJ, 31% efficiency).

The SH and TH pump beams from the harmonics generators are brought to temporal overlap with the white-light seed pulses by two independent variable delay lines (DL1&2) consisting of a pair of mirrors mounted on a translation stage with micrometric positioning. Those dichroic mirrors M5-M9 and M11-M15 are also used to filter out the residual unconverted light from the harmonics crystals. The horizontally polarized pumps and vertically polarized signal are overlapped in two type I, AR-coated BBO crystals. One is cut at $\theta = 33°$ with a thickness of 2 mm (TH-NOPA), the other is 4 mm thick and cut at $\theta = 23.5°$

#209302 - $15.00 USD Received 31 Mar 2014; revised 30 May 2014; accepted 30 May 2014; published 11 Jun 2014

(SH-NOPA). The pumps are focused inside the crystals using the lenses L5&L7 to a spot size of 120 µm FWHM (TH-NOPA) and 150 µm FWHM (SH-NOPA). We estimate the intensity inside the OPA crystals to 70 GW/cm^2.

For seed generation we use the now popular white light generation (WLG) in a YAG window, which has proven to be ideally suited to produce stable continua at high repetition rates [21]. The power of the beam transmitted by the input beam splitter (BS) is adjusted by a variable neutral density filter (VND). 1 to 1.25 µJ (2 W) of FF light is focused by a 50 mm lens (L1) in an uncoated 4 mm thick YAG plate. We obtain a continuum spanning from 480 nm (YAG cut-off [21]) up to the fundamental wavelength of the laser.

This white light is collimated by a silver-coated spherical mirror (M1). The beam is then routed by a set of silver-coated mirrors (M2 to M4). M3 can be inserted in or out of the beam path to switch easily from one to the other NOPA. The signal is then focused in each NOPA crystal by an achromatic lens (AC1&3). The seed beam is focused slightly in front of the NOPA crystals and its size is about twice as big as the pumps inside the crystals in order to improve the beam profile. An additional glass rod (DR) can be placed on the beam path to increase signal dispersion and reduce the amplified bandwidth for some experiments.

Our setup fits on top of a 90x45x20 cm enclosed breadboard, and there is enough free space at the output of both NOPAs to add the chirped mirror compressor described below or an additional second harmonic generator to extend the tunability into the UV.

The full laser system (including NOPA, Tangerine FCPA, T-Pulse master oscillator for synchronization with synchrotrons rep-rate, and beam characterization instruments) fits on a small 1,5x1m optical table mounted on a wheeled frame so as to be transportable to various synchrotron facilities in Europe, like Petra III, ESRF or PSI. The mechanical components have been carefully selected, and for some of them designed in-house, in order to reach the best stability and robustness when the device is moved from one location to the other.

3. Tunable amplification results

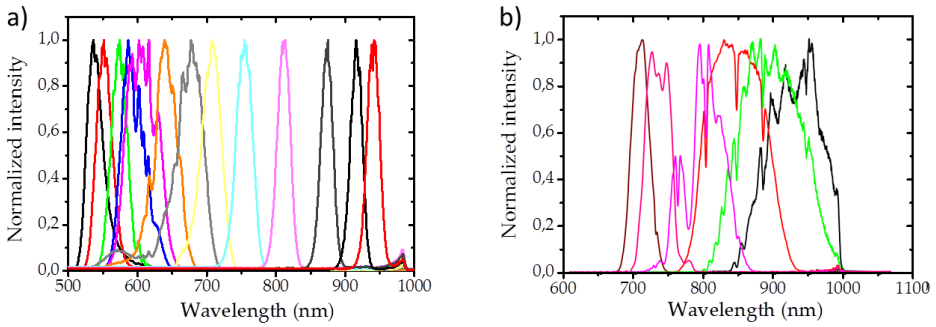

Fig. 2. Spectral tunability of the TH (a) and SH-pumped NOPA (b).

For spectroscopic applications, controlling the spectral bandwidth of the beam is important. Some applications need the broadest amplified spectrum in order to reach ultimate time resolution, while for others a narrow linewidth is needed to excite a defined transition. To get such flexibility, both NOPAs are aligned for broadband amplification at magic angle (internal pump to signal angles are respectively set to 2.6° and 4.7° for SH and TH-NOPA), even if we do not necessarily need ultra-broadband spectra.

In this configuration, the amplified bandwidth is mainly determined by the temporal overlap of the 300 fs pumps with the dispersed seed. By tailoring the continuum's dispersion, it is therefore possible to adjust the spectral width from broadband to narrowband depending on applications. This is done easily and quickly, by insertion of transparent dispersive material. Thanks to magic angle, it suffices to adjust the temporal overlap for tuning the central wavelength of the amplified pulses. For instance, for experiments with our streak

#209302 - $15.00 USD Received 31 Mar 2014; revised 30 May 2014; accepted 30 May 2014; published 11 Jun 2014

camera we often use a 2 cm thick SF10 window (visible range) or a 1 cm thick ZnSe window (NIR range) to reduce the excitation spectrum bandwidth by a factor of about 5 compared to the spectra presented Fig. 2.

Typical amplified spectra are presented Fig. 2. The TH-NOPA operates in the 540 to 950 nm range and the SH-NOPA is tunable from 700 to 1000 nm. As we are using the walk-off compensation (WC) interaction geometry, parasitic SHG of the amplified signal is found at 590 nm and 850 nm respectively for the TH and SH-NOPA, resulting in a gap in the amplified spectrum. It is due to the fact that the phase-matching angle is the same for SHG and OPA at those wavelengths. It could be avoided by using the non-walk-off compensation (NWC) configuration (180° rotation of the crystal around the beam axis of propagation) at the expense of a lower beam profile quality [22].

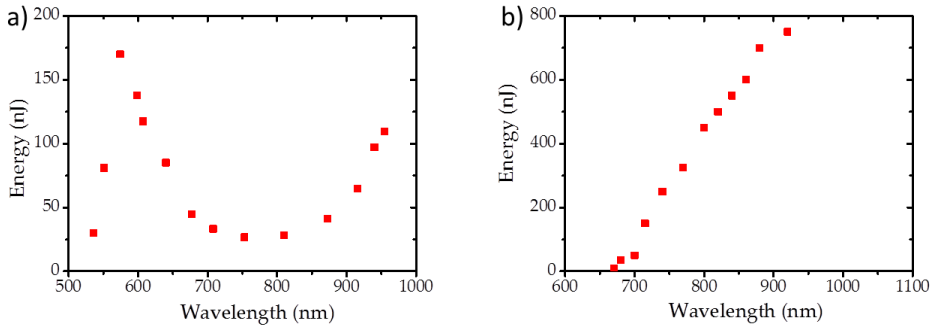

Fig. 3. Output energy of the TH (a) and SH-pumped NOPA (b).

The output energy of the two NOPAs at 2 MHz operation is shown Fig. 3. It is higher than 25 nJ from 500 to 900 nm for the TH-NOPA with a maximum of 170 nJ at 580 nm (6.8% conversion efficiency). The energy is higher than 100 nJ from 710 to 1000 nm for the SH-NOPA with a maximum of 750 nJ at 920 nm (18.7% conversion efficiency). The efficiency of the TH-NOPA is rather low due to the lower intensity inside the crystal. Increasing the intensity to 100 GW/cm^2 eventually results in damage of the BBO crystal due to thermal gradient inside the crystal.

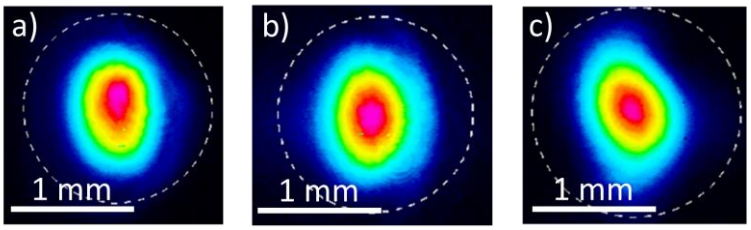

Fig. 4. Typical amplified beam profiles: TH-NOPA at 640 nm and 2 MHz (a), same at 200 kHz (b) and SH-NOPA at 820 nm and 2 MHz (c).

Amplified beam profiles at 2 MHz are slightly elliptical (Fig. 4). Ellipticity is better when the repetition rate is reduced using the external AOM of the fiber pump laser. The beam diameter is constant regardless of the repetition rate in the vertical direction, while it is changing in the other (phase-matching direction). We thus attribute this ellipticity change to the coupling between the thermal gradient inside the amplifying crystal and the thermally sensitive phase-matching.

The TH-NOPA is by far the most sensitive to these thermal effects. It has been reported that idler and pump absorption is the main contribution to thermal heating of nonlinear crystals, and that absorption in the crystal coating can increase the heating of the crystal by 25% [23]. In our case, heating is partly due to two-photon absorption (TPA) of the 343 nm

#209302 - $15.00 USD Received 31 Mar 2014; revised 30 May 2014; accepted 30 May 2014; published 11 Jun 2014

pump in BBO: at an intensity of 100 GW/cm^2 (damage intensity), TPA of the UV pump is estimated to 15%. Additional absorption in the crystal coating is also possible: using an uncoated crystal might reduce heating and allow for a higher pumping intensity and conversion efficiency despite the increased Fresnel losses.

Thanks to its external modulator, the Tangerine pump laser allows changing the repetition rate at will without changing the energy per pulse and the intensity inside the crystals. However, the change in thermal load inside the crystals (including the YAG window) implies that the output energy will change depending on the repetition rate, so it might be needed to optimize the focusing inside the OPA crystals to get optimal efficiency. We also need to increase the energy focused in the YAG window due to thermal heating, from 1 µJ at 200 kHz to 1.25 µJ at 2 MHz, using the variable density filter VND. When the energy is fixed to 1 µJ and the repetition rate to 2 MHz, we can see an initial bright white light at the opening of the laser shutter, but the WL intensity then drops very quickly as the YAG plate is heating up. When the continuum is generated, 15% of the laser power is indeed absorbed in the YAG plate due to nonlinear absorption. We did not notice any change in the spectral width while changing the repetition rate.

The output power of the NOPA is remarkably stable. For example, long-term fluctuations of the SH-NOPA are 0.5% RMS over a recording period of 90 minutes (Fig. 5) and 1.3% peak-to-peak. Enclosing the breadboard is very important to get stable output power, especially for the UV-pumped NOPA. When the enclosure is opened, the TH-NOPA behaves as a thermometer: the output power follows exactly the evolution of the room temperature.

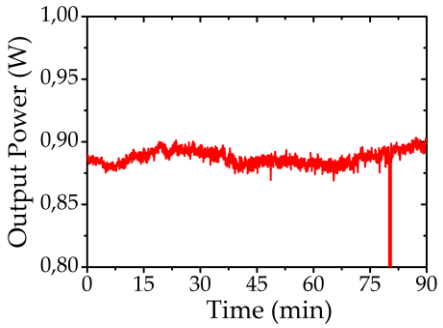

Fig. 5. SH-NOPA power fluctuations measured over 90 minutes. The drop-out corresponds to an opening of the laser shutter.

4. Broadband amplification results

As the NOPAs are in a magic-angle configuration, the amplified bandwidth is only determined by the white-light chirp. In the previous section, we have demonstrated tunable amplification for both OPA but it could also be very interesting for some experiments to generate those ultra-broadband spectra followed by appropriate compression to few optical cycle duration. To do so, the optical setup has to be modified slightly to reduce the seed chirp and match signal and pump pulse durations. In our setup, more than half the continuum dispersion is due to the thick achromatic lenses AC1&AC3 used to focus the seed inside the NOPA crystals. To reduce seed dispersion we have removed those two lenses and mounted the spherical mirror M1 on a short translation stage for focusing the continuum. This solution is however less flexible and was chosen for demonstration purposes only: as the optical path length is not the same for the SH and TH-NOPA, the position of this mirror has to be adjusted each time one switches from one NOPA to the other in order to place the continuum focus at the right point. A better solution could be to replace the achromatic doublets by simple plano-convex lenses made in a low dispersive material such as calcium fluoride.

After adjusting the pump delays for temporal overlap with the seed, we observed broadband amplification for both OPAs (Fig. 6). The non-collinear angle was adjusted as the

#209302 - $15.00 USD Received 31 Mar 2014; revised 30 May 2014; accepted 30 May 2014; published 11 Jun 2014

amplified bandwidth can be even larger for a slightly smaller angle compared to magic angle [24]. In this configuration, the amplified spectrum is 225 nm broad ($1/e^2$) at a central wavelength of 570 nm in the TH-NOPA, supporting a Fourier limited pulse duration of 4.2 fs (2.2 optical cycles). It is 350 nm broad ($1/e^2$) at a central wavelength of 845 nm in the SH-NOPA, supporting a TF pulse duration of 5.4 fs (1.9 optical cycles). In both cases a hole in the amplified spectrum is visible at a wavelength of 585 nm for the TH-NOPA and 850 nm for the SH-NOPA due to the same parasitic SHG already reported and explained in the tunable configuration. The broadband spectrum is more modulated in the SH-NOPA compared to the TH-NOPA, probably due to parasitic sum-frequency mixing [18] and to the structuration of the white-light spectrum close to the fundamental frequency. The output energy is the same as the maximum obtained in the tunable configuration.

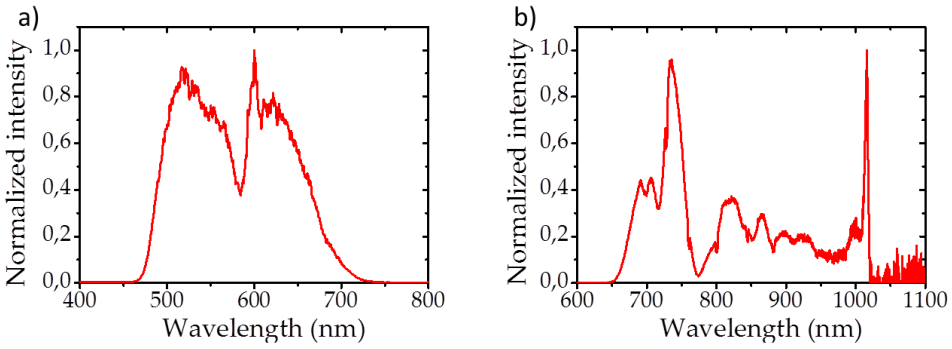

Fig. 6. Ultra-broadband spectrum generated in the TH (a) and SH pumped NOPA (b) at magic angle.

6. NOPA compression

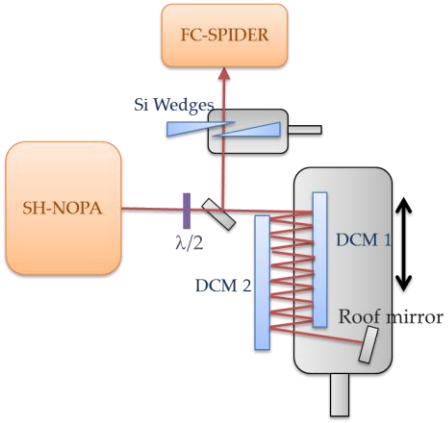

Fig. 7. SH-NOPA chirped mirrors compression setup.

In the narrowband operation suitable for wavelength tuning (Fig. 2) the amplified spectra support transform limited (TF) pulse durations below 30 fs from 500 to 750 nm with a minimum of 11.5 fs at 620 nm for the TH-NOPA, and pulse durations below 30 fs from 700 to 1000 nm with a minimum of 14 fs at 870 nm for the SH-NOPA (Fig. 8). The TF pulse durations grow rapidly at the vicinity of the spectral cutoff due to the asymptotic shape of the phase-matching curves when the idler starts to be absorbed. Amplified pulses at the output of both NOPAs have basically the pulse duration of the pump beam, much longer than those ultrashort TF-limited durations. A compression setup is therefore needed to compensate for the phase acquired by the signal during its propagation from the white light YAG plate to the experiment.

#209302 - $15.00 USD Received 31 Mar 2014; revised 30 May 2014; accepted 30 May 2014; published 11 Jun 2014

Many options could be considered to compress the output pulses of a NOPA. A fused-silica prism compressor [25] is easy to handle and adaptable to different central wavelengths. But fused-silica prism compressors are bulky when the GDD to compensate for is high. In our NOPA GDD = 1920 fs^2 at 900 nm, which requires an apex-to-apex prism distance of about 1.2 m. Compactness can be improved using more dispersive material like SF-10 prisms, at the expense of a large uncompensated third-order dispersion (TOD).

A broadband double chirped mirrors (DCM) compressor is an appealing alternative, with its high throughput, compactness and user-friendliness [26]. Moreover, new broadband DCM designs are also able to compensate for TOD, enabling shorter pulse durations compared to prism compression. We have opted for such a chirped-mirror compressor to compress our SH-NOPA with a spectrum centered at 800 nm. The main advantage for us is the possibility to fit the compressor directly inside the NOPA enclosure in order to preserve the high stability of our system.

For the TH-NOPA, convenient broadband DCMs with high enough dispersion in the visible spectral range are presently unavailable "off-the-shelf". A more costly custom design would of course be the best long-term solution. For demonstration purpose, we present here compression results of the TH-NOPA with a simple fused-silica compressor, keeping in mind that the compressed pulse duration could be significantly shorter with the availability of TOD compensated DCM.

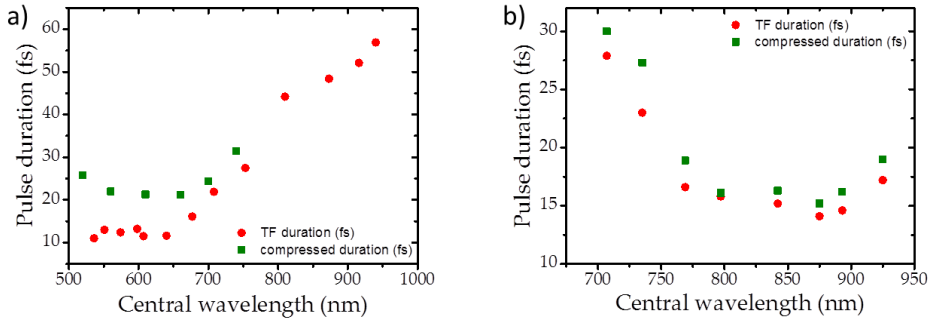

Fig. 8. Transform limited (red dots) compared to measured pulse duration (green squares) after compression of the TH-NOPA with a fused silica prism compressor (a) and SH-pumped NOPA with a chirped mirrors compressor (b).

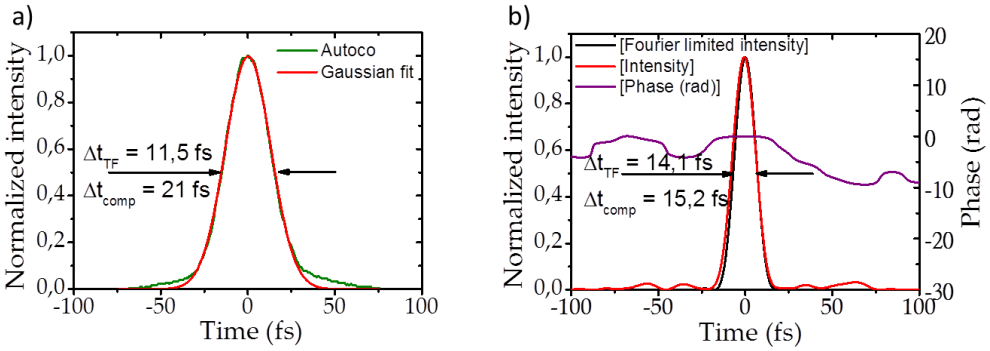

Fig. 9. a) Shortest autocorrelation traces (green) and Gaussian fits (red) of the TH-NOPA. b) FC-SPIDER temporal profile reconstruction of the shortest SH-NOPA compressed pulses at 875 nm for the on-purpose limited spectral bandwidth obtained in the tunable operation mode (Fig. 2).

The SH-NOPA compressor chirped mirrors are designed for the 630-970 nm spectral range (Femtolasers). They came in a large size of 80x20 mm allowing multiple bounces. Each double bounce compensates 60 fs^2 at 900 nm as well as the third order phase. The compression setup is sketched Fig. 7. Distance between the mirrors is set to 1 cm and

#209302 - $15.00 USD Received 31 Mar 2014; revised 30 May 2014; accepted 30 May 2014; published 11 Jun 2014

incidence angle is about 10°. The maximum number of bounces on a row is 20 and a roof mirror is used to add a second pass. One chirped mirror is fixed while the second one is mounted on a translation stage (50 mm travel range) together with the roof mirror in order to quickly adjust the number of bounces. A pair of fused silica wedges is placed at the output of the compressor for fine adjustment of the dispersion (only used for the broadband NOPA configuration). With 80 bounces max, aligning both mirrors in perfect parallelism is very challenging. Any tiny misalignment led to beam pointing issues when changing the number of bounces. The compressor, without wedges, fits in a 15x10cm^2 box, which is quite an improvement over the 1.2 m long prism compressor. The compressed pulses are then characterized with APE's FC-SPIDER.

We concluded that the optimal number of bounces is 64 (32 double bounces, 16 on a row) for the tunable NOPA configuration, compensating a total GDD of 1920 fs^2 at 900 nm. The number of bounces is the same regardless of the amplified wavelength, i.e. no realignement is needed when tuning the NOPA. We measure a throughput of 65%. The compressed pulse duration is lower than 30 fs from 700 nm to 950 nm with a minimum of 15.2 fs at 875 nm (Figs. 8 and 9). It is 1.1 to 1.2x the Fourier limit on the full spectral range.

For the TH-NOPA, pulse durations at the output of the prism compressor are below 32 fs from 520 to 750 nm with a minimum of 21 fs at 610 nm. This is 1.3 to 2x the Fourier limit, larger at shorter wavelengths due to increasingly high uncompensated TOD.

Finally, we tested the DCM compressor with the broadband SH-NOPA configuration. As the amplified beam dispersion is reduced, only 40 bounces are needed for optimum compression, increasing the throughput of the compressor to 73%. We optimized carefully the amplified spectrum to obtain the shortest pulse duration. Fine tuning of the dispersion was done by inserting fused silica wedges on the beam path. We succeeded to compress the pulses to 6.0 fs (2.1 optical cycles) with TF duration of 5.4 fs (Fig. 10).

This is to our knowledge the shortest pulse duration obtained from a compact white light seeded MHz NOPA. This is a clear improvement over previously published similar works, where pulse duration was limited to 9.7 fs at 1 MHz [27]. Slightly shorter pulse durations have been demonstrated earlier, but at repetition rates one order of magnitude lower and using a more complex and expensive setup including CEP-stabilized octave-spanning oscillator: 5 fs at 150 kHz [18] or 4.6 fs at 200 kHz [19], the first one including a pulse shaper.

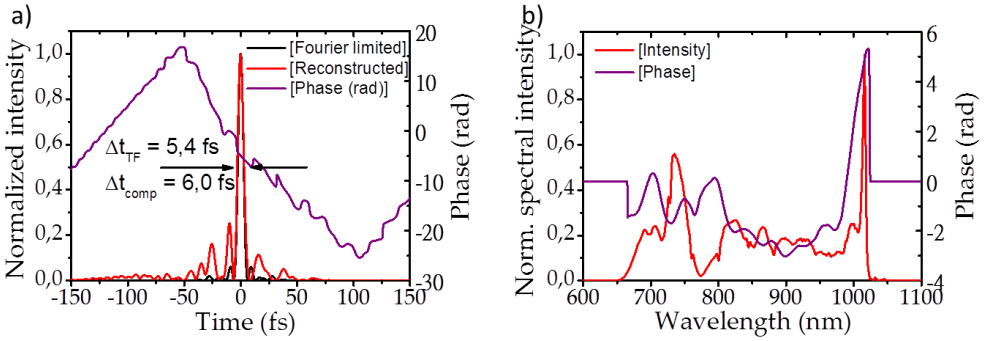

Fig. 10. FC-SPIDER temporal and spectral characterization of the ultrashort 6,0 fs pulses at 840 nm.

6. Conclusion

We have demonstrated the generation of tunable pulses between 520 and 1000 nm with pulse durations in the range 14 to 30 fs and energies from 25 to 750 nJ at a high repetition rate of 2 MHz. With minor adjustments, our NOPA can also be operated in a broadband configuration able to generate 6.0 fs pulses at 850 nm as well as a spectrum supporting 4.2 fs FT pulses at 570 nm. This is the first demonstration of the generation of two optical cycle pulses at MHz repetition rate from a bulk white-light seeded NOPA, without any pulse shaping.

#209302 - $15.00 USD Received 31 Mar 2014; revised 30 May 2014; accepted 30 May 2014; published 11 Jun 2014

In addition, the future availability of broadband chirped mirrors with high enough dispersion in the visible to avoid too many bounces should allow us to demonstrate the generation of two optical cycle pulses in the visible from our MHz TH-NOPA.

Until now, parametric devices were specialized systems able either to generate tunable pulses or broadband pulses, at fixed repetition rates and in specific spectral ranges. Our new modular design offers an all-in-one solution able to meet most users' demands with only minor adjustments.

Besides this very high flexibility of every laser parameter, the use of a white-light seed allows for a much more compact setup compared to complex systems based on octave-spanning Ti:Sa oscillators which are also able to deliver two optical cycle pulses. The NOPA housing fits in a 90x45cm footprint, and the full laser system on a 1x1.5 m optical table (including the optional synchronization setup for experiments at synchrotron radiation facilities). Using a more compact pump laser with the same performances at 2 MHz, like the *Satsuma* from Amplitude Systèmes, the full laser system could even fit on a 45x140 cm breadboard. The compactness and robustness of our mechanical design allows for very high beam stability important for applications.

The technology of femtosecond MHz Ytterbium lasers is progressing quickly. New lasers are already commercially available which are able to deliver even higher output power, up to 50W. It could allow scaling the output energy of our MHz NOPA device to the µJ range, but with an increased difficulty to deal with the high thermal load inside nonlinear crystals. This is especially the case for the TH-pumped NOPA as discussed in section 3. New strategies will be needed to increase the pump power without damaging the crystals, like water-cooling and use of uncoated crystals.

We have already intensively used our NOPA for spectroscopic applications making use of the large tunability of these sources from near-UV to near-IR, and the ability to control the repetition rate (important for molecular systems with slow ground state recovery due to long-lived triplet states). The NOPA pulses excited a large variety of organic and inorganic fluorescent samples the emission of which was recorded using a streak camera with 10 ps time resolution(C 10627, Hamamatsu) [28]. During these experiments we had the opportunity to use the device in all possible configurations, using either SH or TH-NOPA, adding seed dispersion to narrow the amplified bandwidth, removing seed dispersion to get broadband spectrum, or adding a SHG module at the output to generate UV light, with repetition rates from 5 Hz to 2 MHz. The high long-term stability of the sources (Fig. 5) turned out to be another key advantage. In addition, drift of the electronic synchronization between the Tangerine and the streak camera was found to be lower than 1ps over more than 10 hours of acquisition in photon counting mode.

Our 2 MHz prototype will now be synchronized with synchrotron beams in order to perform time-resolved optical pump/X-Ray probe experiments. Beam time is planned at the European Synchrotron Radiation Facility in Grenoble and Petra III at Desy in Hamburg. The laser source will be located inside the X-ray hutch, thus inaccessible to users. In this context, remote control of a motorized pump-seed delay stage and crystal rotation stage for wavelength tuning is an obvious improvement to be easily implemented. Thanks to the 2 MHz repetition rate, X-ray time resolved studies will now benefit from an improved data acquisition speed as well as a better signal-to-noise ratio. We foresee that this kind of instrument will become a standard tool on many synchrotron beamlines in the future.

Acknowledgments

The authors are grateful to APE Berlin and particularly G. Stibenz for the loan of a FC-SPIDER, and to Femtolasers for the generous loan of the chirped mirror compressor. JN thanks Y. Zaouter from Amplitude Systèmes for helping with the laser system. We acknowledge financial support from the European Commission 7th FP under grant 315744 (FLAME). CB&JN acknowledge funding funding by the EU-funded Cluster of Research Infrastructures for Synergies in Physics (CRISP) project, CB also the Deutsche Forschungsgemeinschaft via SFB925.

#209302 - $15.00 USD Received 31 Mar 2014; revised 30 May 2014; accepted 30 May 2014; published 11 Jun 2014